setting and subject the wires to a radial compression. It is the frictional force acting on the wire as a result of this compression, rather than any bond formed between the wire and the matrix, which supplies the maximum force opposing pull-out in our specimens.) This process of "plastic release" then propagates along the wire towards the embedded end until the wire is able to pull out. The residual length of wire that is strongly gripped by the matrix remains constant as the wire is pulled out, up to the point where it reaches the simulated crack, so that the pull-out force also remains constant up to this point. This behaviour resembles that proposed for the pull-out of a long elastic fibre by Takaku and Arridge [2], where the lateral contraction of the wire given by Poisson's ratio serves to release it from the matrix and sets a limiting value to the force required to pull the fibre out. We suggest that when the limiting pull-out stress given by Takaku and Arridge exceeds the yield stress of a wire which is capable of substantial uniform plastic elongation, the wire is released by plastic deformation and pulled out at a limiting stress given by the flow stress at the plastic strain needed to obtain release. For nickel wires in our cases the limiting pull-out stress for elastic behaviour exceeds the ultimate tensile strength of the wire, and the work-hardened wire, which is not capable of sufficient further uniform plastic elongation to release it from the matrix, fractures when a critical length is exceeded.

To check the above explanation, the lengths and stress-strain curves of the pulled-out portions of the annealed nickel wire, pulled from the resin matrix, were measured. Increases in length of between 4% and 5% occurred, and the yield stress in tension was equal to the flow stress of an annealed wire at a plastic strain of 7%. The nominal stress at yield of a pulled-out wire, 305 N mm^{-2} was somewhat less than the limiting pull-out nominal stress of 350 N mm^{-2} (Fig. 2). These results suggest that the wire undergoes an inhomogeneous plastic elongation during pull-out, most severe at the crack position, so that the tensile test sampling a region of wire between the crack position and the end records a slightly lower yield stress than the pull-out stress. If the hardening of the wire at the crack position is attributed entirely to plastic elongation, a strain of about 9% at this point is implied.

The observations described in this note suggest in designing composites of the wire-reinforced cement type, there may be advantage in employing wires having a high work-hardening rate and a uniform elongation to failure of, say, 10%, in order to maximize the work of fracture of the composite.

References

1. A. H. COTTRELL, *Proc. Roy. Soc.* **A282** (1964) 3.
2. A. TAKAKU and R. G. C. ARRIDGE, *J. Phys. D: Appl. Phys.* **6** (1973) 2038.

Received 29 August
and accepted 9 September 1974

J. MORTON
G. W. GROVES
Department of Metallurgy and Science of Materials, Oxford University, UK

The optical reflection transform method

The purpose of this short note is to present a simple diffraction explanation for the patterns created when a collimated beam of light is reflected back from a material having a crystallographic topography. At its simplest, the technique is a direct copy of the back-reflection Läue technique with the X-ray beam replaced by a light beam.

The technique has a long history, dating back to its conception by Chalmers [1] who used it to measure the angle of twinning in deforming tin crystals. Later workers, among them Cocks *et al.* [2] and Yagi *et al.* [3], have used the method and have coined various terms such as "laser reflectogram", "light figure method" and "reflection pattern method" to describe it, but have, it is felt here, incorrectly or incompletely interpreted the resulting patterns. From the simple analysis presented here the term, if a term is necessary at all, "optical reflection transform method" would appear to be more appropriate.

Purely to illustrate the inadequate interpretation of the reflected light patterns that Cocks *et al.* and other workers have made, reference is made to Fig. 2 of the article on the laser reflectogram method by Cocks *et al.* [2]. They were studying the crystallographic nature of the pits created by etching in crystals of silicon carbide. Cocks *et al.*

correctly related the hexagonal symmetry of the pattern to the hexagonal etch pits and suggested that the presence of lines rather than spots was due to a diffraction grating effect (*sic*) from the steps in the etch pit structure. They did not however explain why there is only one hexagonal pattern rather than many nor why the arms are of limited length. Yagi *et al.* [3] merely explained their patterns by saying that the etch pit surfaces (of germanium) acted as mirrors.

From a diffraction theory point of view the transmission and reflection diffraction patterns of an array of objects will be identical in shape and will have relative intensities determined by the relative scattering powers for transmission and reflection of the objects. This can be shown qualitatively as follows, using Fig. 1 to define some of the necessary quantities.

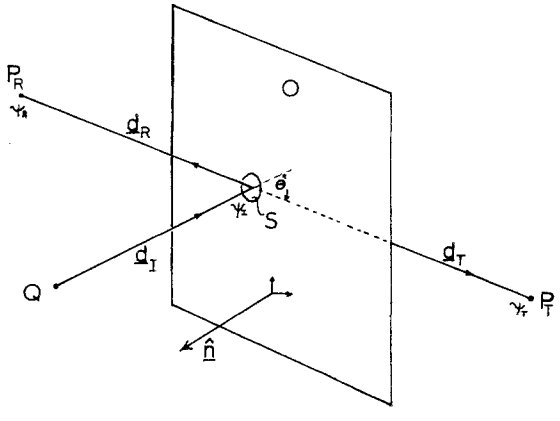

Figure 1 Schematic diagram to illustrate the diffraction of light from an object in both transmission and reflection. The distances and legend are used in the text.

Consider the amplitude observed at points P_R and P_T arising from coherent light emitted from a point source Q and scattered by a plane object at O. Suppose that if an element of area dA at point S on the object is illuminated by a wave ψ_I the point acts as a coherent secondary emitter of strength $f\psi_I dA$ where f is the scattering function of O at the point S. For the purposes of simplification the angular variation of f is neglected here. The subscript T or R refers to whether the scattering function is for transmission or reflection.

Writing the scalar wave emitted from the source Q which has strength W_I as a spherical wave

$$\psi_I = \frac{W_I}{d_I} \exp(-ikd_I)$$

the point S acts as a secondary emitter of strength, $W = f\psi_I dA$. The contributions of ψ received at P_T and P_R are then

$$d\psi_T = f_T \Psi_I \exp(-ikd_T) \frac{dA}{d_T}$$

$$= f_T dA \frac{W_T}{d_I d_T} \exp[-ik(d_T + d_I)]$$

and similarly

$$d\psi_R = f_R dA \frac{W_R}{d_I d_R} \exp[-ik(d_R + d_I)] .$$

The total amplitudes received at P_T and P_R are then the integrals of these two expressions over the area of the object. For a parallel incident beam of light and a planar object, the integrals have the familiar fourier transform format

$$\psi = \int_{\text{plane}} f(\mathbf{r}) \frac{1}{d} \exp(-ikd)\, d(\mathbf{r})$$

for both reflection and transmission providing the appropriate scattering function and distances d are used. (Constant factors over the object plane have been omitted from the integral.)

From this it should be clear that the normal diffraction properties apply in the formation of the reflected light patterns, namely, the symmetry of the reflection pattern relates to the symmetry in the object and the spacings in the diffraction plane are inversely related to those in the object plane.

Thus the reflection pattern of a collection of hexagonal etch pits, each of identical size and all having corresponding edges parallel to one another will be six spots arranged on a hexagon. If the etch pit's edges remain crystallographically related but the size of the pits varies the spots will be smeared out along lines at 60° to one another, passing through the positions of the spots and the centre point. Furthermore, the intensity along the lines will be determined by the size distribution of the etch pits.

Examination of Fig. 2 of Cocks *et al.* shows, (a) that the corresponding edges of the etch pits are parallel, (b) the size of the pits does vary, and (c) there appears to be a minimum size of etch pit. The star shaped optical reflection transform pattern can thus be completely explained including the maximum length of the arms.

As a test for this diffraction interpretation,

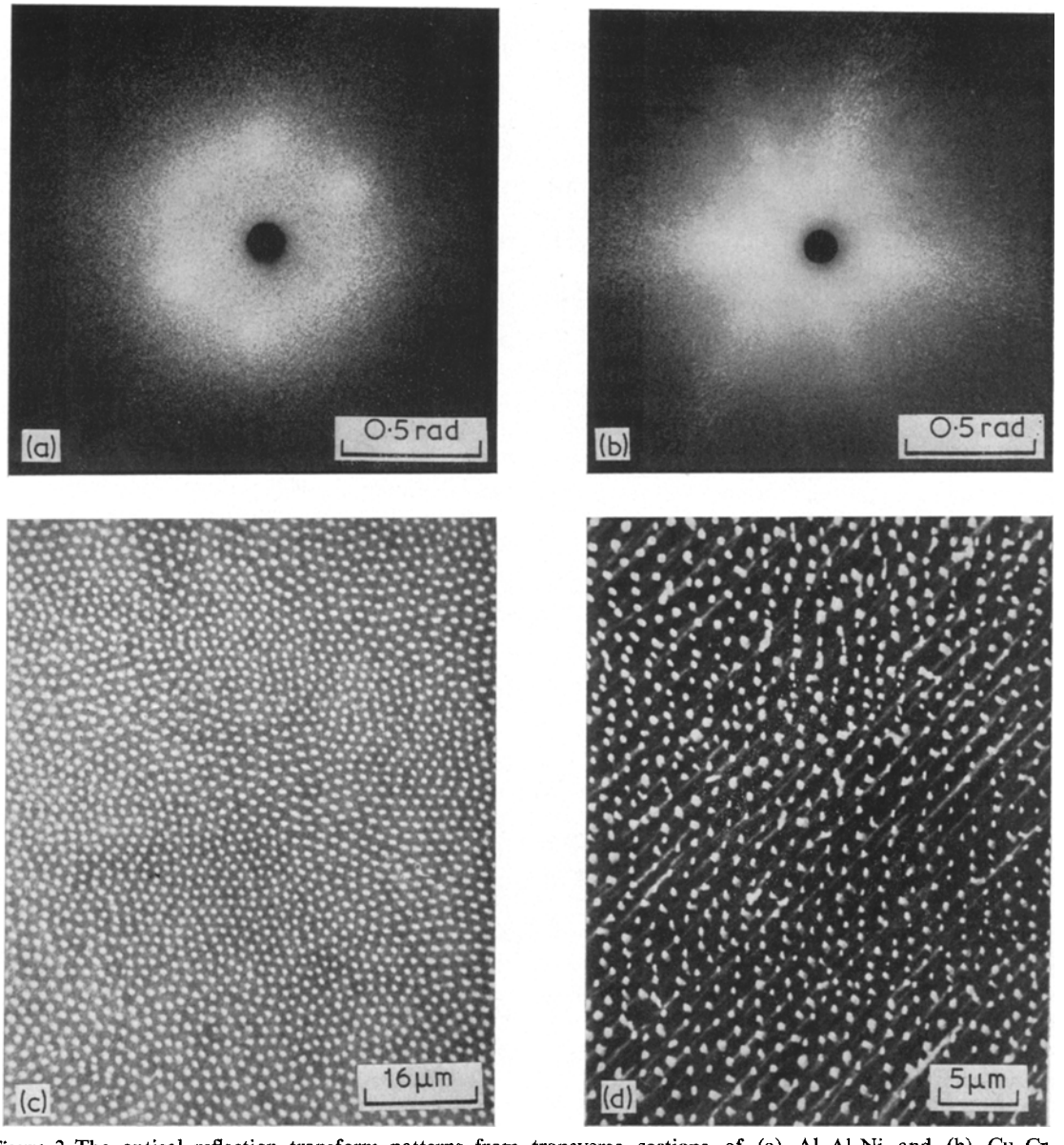

Figure 2 The optical reflection transform patterns from transverse sections of (a) Al–Al_3Ni and (b) Cu–Cr illuminated with a helium-neon laser (6328 Å). (c) and (d) Scanning electron micrographs of the areas of the alloys in (a) and (b) respectively, giving rise to the above patterns.

transverse sections of Cu–Cr and Al–Al_3Ni eutectic alloys were compared by the optical reflection transform method. The Al–Al_3Ni alloys can be grown to form a more uniform fibre lattice than can the Cu-Cr alloys, although both lattices are close to being hexagonal (trigonal) in cross-section. Fig. 2 are the patterns from a Cu–Cr alloy and an Al–Al_3Ni alloy together with scanning micrographs of the examined areas. The transverse (to the fibre directions) sections were prepared by first polishing and then selectively etching to leave the ends of the fibres standing proud of the alloy surface. The more regular fibre lattice in Al–Al_3Ni is borne out by the more spot-like optical reflection transform from that alloy. (The Al–Al_3Ni specimen was kindly

provided by H. Bishop of the Department of Metallurgy, Cambridge).

The optical reflection transform method has a number of advantages over the normal metallographic examination of surfaces. Firstly, it provides a very rapid and easy detection of the presence of surface symmetries, especially for objects whose spacing is commensurate with the wavelength of light. Secondly, it enables a very rapid and quite accurate determination of the mean spacing of objects to be made. This is useful in analysing eutectic growth structures and measuring the inter-particle spacing. Thirdly, the technique is equally valid for small or large area (0.01 to 100 mm^2) examination.

Acknowledgements

The work described here was carried out at the Cavendish Laboratory, Cambridge and it is a pleasure to acknowledge the financial support provided by the National Physical Laboratory. It is also a pleasure to acknowledge the helpful discussions held with other members of the Metal Physics group of the Cavendish.

References

1. B. CHALMERS, *Proc. Phys. Soc.* **47** (1935) 733.
2. F. H. COCKS, B. N. DAS and G. A. WOLFF, *J. Mater. Sci.* **2** (1967) 470.
3. H. YAGI, K. SHIMAKAWA and N. TSUKADA, *Proc. IEEE* **57** (1969) 2156.

Received 5 September
and accepted 23 September 1974

DAVID R. CLARKE*
National Physical Laboratory
Teddington, Middlesex, UK

*Present address: Lawrence Berkeley Laboratory, University of California, Berkeley, California 94720, USA.

Density changes during creep of polycrystalline MgO

Cavities and cracks have been observed to form on grain boundaries during high temperature creep of ceramic materials [1-6]. However, this aspect of the creep behaviour of ceramics has received little attention compared with that devoted to the study of crack development during creep of metals and alloys [7, 8]. Furthermore, intercrystalline fracture of metallic materials has generally been studied using tensile creep conditions, whereas most of the work on creep of ceramics has been carried out using bend or compression testing procedures. In the present investigation, a technique which has frequently been employed to follow crack formation with metals, namely, the accurate measurement of density changes during creep [9-12], has been combined with microstructural studies in order to examine the development of grain-boundary cracks during compressive creep of polycrystalline MgO.

The present work was carried out using magnesia specimens (4.25 mm diameter and 6.4 mm long) having 94 to 96% theoretical density, 99.85% purity and 10 to 14 μm average grain diameter. Details of the material preparation [13], the constant stress creep equipment [14] and the differential weighing technique used to measure the specimen density [12] have been given elsewhere. With the small MgO specimens used, the fractional density change, $\Delta\rho/\rho$, could

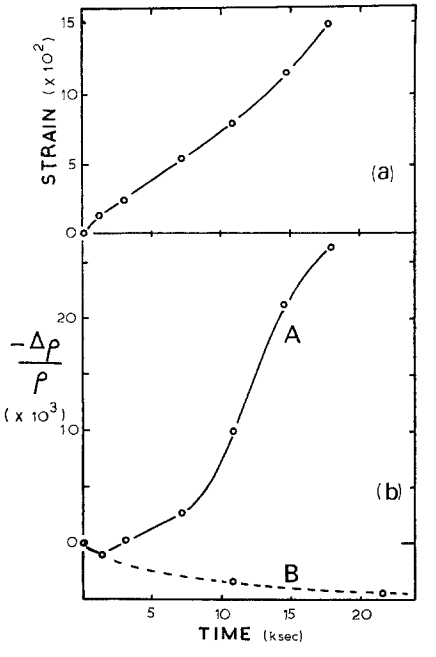

Figure 1 (a) Variation of creep strain with time for polycrystalline MgO at 96.2 MN m^{-2} and 1596 K. (O indicates points at which density determinations were carried out.) (b) Fractional change in specimen density with time at 1596 K during creep (curve A) and in the absence of an applied stress (curve B).